Magnetization and Critical Fields of Superconducting $SrTiO_3$

E. AMBLER, J. H. COLWELL, W. R. HOSLER, AND J. F. SCHOOLEY*
National Bureau of Standards, Washington, D. C.
(Received 7 March 1966)

Magnetization curves from $T=0.15°K$ to T_c have been measured for two specimens of semiconducting $SrTiO_3$ of electron density about 10^{20} cm^{-3}. Magnetic hysteresis was observed in each case. The temperature dependences of the first and second critical fields have been measured and compared with the derivations of Maki. The heat capacity has been measured down to 0.3°K for one specimen, yielding γ, the coefficient of the linear term, and an independent value of T_c at the upper part of the specific-heat anomaly. The Ginzburg-Landau κ is shown to vary inversely with the electronic mobility.

I. INTRODUCTION

OUR experimental investigations on semiconducting $SrTiO_3$ for the occurrence of superconductivity were motivated by theoretical predictions[1] made on the basis of the normal-state properties,[2,3] and by preliminary experimental results available to us on GeTe.[4] We have shown already that both dc resistance measurements and ac magnetic-susceptibility measurements indicate the occurrence of superconductivity in reduced $SrTiO_3$,[5] and we have measured the dependence of the superconducting transition temperature upon carrier concentration.[6]

Efforts to characterize the superconductivity of $SrTiO_3$ as completely as possible and to correlate the results with theory have been in progress for some time. A great deal of information can be obtained about a superconductor by measurements of its magnetic moment as functions of applied field and temperature; accordingly, a sensitive vibrating-coil magnetometer useful for specimens down to $T\approx0.1°K$ was built. This apparatus will be discussed only briefly, since a detailed description of it appears elsewhere.[7] Further information can be obtained by measuring the heat capacity, and this measurement has been made for one specimen down to 0.3°K.

A wide variety of specimens is available for the measurements described above. As discussed in Ref. 6, superconductivity is observed in samples of carrier concentration n_c from 10^{18} to 10^{21} cm^{-3}. As n_c is increased in this range, the critical temperature reaches a maximum value and then falls off. In order to minimize the effect of errors in sample temperature measurement and of any sample inhomogeneity, specimens were chosen for the initial magnetization and heat-capacity measurements with $n_c=1$ to 2×10^{20} cm^{-3}, corresponding to the peak in T_c.

$SrTiO_3$ can be made semiconducting in two ways, doping during growth with an impurity, for example Nb, or partial reduction at elevated temperatures after growth.[2] Above 5×10^{19} carriers cm^{-3}, niobium-doped specimens exhibit a low-temperature electronic mobility some 2.5 times that seen in reduced specimens of the same carrier concentration. As will be discussed in Sec. IV, the value of κ, the Ginzburg-Landau order parameter, can be expected to vary approximately inversely with electronic mobility for superconductors in which the electronic mean free path is less than the coherence length, so that it was attractive to measure the magnetization of both a niobium-doped and a reduced specimen.

This paper describes the results of magnetization measurements on a niobium-doped single-crystal specimen (Nb10) of $n_c=1.7\times10^{20}$ cm^{-3} and 4.2°K mobility $\mu=600$ cm^2 V^{-1} sec^{-1} and on a reduced single-crystal specimen (HR24) of $n_c=1.0\times10^{20}$ cm^{-3} and μ (4.2°K) $=225$ cm^2 V^{-1} sec^{-1} from 0.15°K to T_c and the results of heat-capacity measurements on a niobium-doped polycrystalline specimen (Nb13) of $n_c=1.4\times10^{20}$ cm^{-3} from 0.3 to 4°K.

II. MAGNETIZATION MEASUREMENTS

A. Apparatus

Observation of the magnetic moment of $SrTiO_3$ specimens involved two problems. First, the specimen must be cooled to $T<T_c$ and T must remain reasonably constant during any measurement. Because of the small specimen heat capacity and limited thermal contact, this condition implied a low rate of heat dissipation at the specimen by the measuring apparatus. Second, preliminary ballistic-galvanometer measurements had indicated that the first and second critical fields were a few oersted and a few hundred oersted, respectively, as expected from the predicted value of κ.[5] This condition implied that the measuring apparatus must detect 10^{-5} to 10^{-6} emu over the range $H=0-1000$ Oe.

In order to satisfy these requirements, a vibrating-coil magnetometer was designed for use with a modification

* Supported in part by The Advance Research Projects Agency.
[1] M. L. Cohen, Phys. Rev. 134, A511 (1964).
[2] H. P. R. Frederikse, W. R. Thurber, and W. R. Hosler, Phys. Rev. 134, A442 (1964).
[3] A. H. Kahn and A. J. Leyendecker, Phys. Rev. 135, A1321 (1964).
[4] The initial example of superconductivity in a semiconductor was GeTe, reported by R. A. Hein, J. W. Gibson, R. Mazelsky, R. C. Miller, and J. K. Hulm, Phys. Rev. Letters 12, 320 (1964).
[5] J. F. Schooley, W. R. Hosler, and M. L. Cohen, Phys. Rev. Letters 12, 474 (1964).
[6] J. F. Schooley, W. R. Hosler, E. Ambler, J. G. Becker, M. L. Cohen, and C. S. Koonce, Phys. Rev. Letters 14, 305 (1965).
[7] R. S. Kaeser, E. Ambler, and J. F. Schooley, Rev. Sci. Instr. 37, 173 (1966).

of the adiabatic demagnetization apparatus described earlier.[6] The detailed operation of the magnetometer has been discussed elsewhere,[7] so that only a brief description of the experimental arrangement will be given here. Figure 1 shows that part of the specimen mount and magnetometer which is enclosed by the tail of the liquid-helium Dewar. The Pyrex vacuum jacket V is connected through a Kovar seal Q to the exchange-gas pumping line. The electrical leads inside V and the mechanical support H are thermally grounded by spring fingers F at about 1°K, by contact with the thermal guard pill L_1 at about 0.14°K, and by contact with the chrome potassium alum-epoxy resin pill L_2. The specimen S and a chrome potassium alum thermometer K are connected through greased junctions to copper wires embedded in L_2. Mutual-inductance coils I were monitored by a Hartshorn bridge[8] operating at 210 cps. A length of resistance wire is wrapped on S. The magnetometer assembly is fastened to V by loudspeaker spiders at Z_1, Z_2, and Z_3. A pair of coils M_1 and M_2 wound in magnetic opposition are vibrated vertically by a vibration generator connected through vacuum bellows to the stainless-steel drive tubes shown above Z_3. The signal from $M_{1,2}$ depends directly on the magnetic moment of the specimen, and on the vibration amplitude. The amplitude dependence is eliminated by use of a compensating coil pair mounted above the Dewar. This pair is connected in electrical series with $M_{1,2}$ and vibrates about a small solenoid which functions as a variable magnetic dipole. Thus the dipole current required to null the $M_{1,2}$-compensator signal is directly proportional to the specimen magnetic moment and independent of vibration amplitude. A preamplifier and a lock-in amplifier were used to observe the null point. Steady magnetic fields up to about 50 and 1500 Oe could be applied by internal solenoid V and by an external solenoid (not shown), respectively. The external solenoid was compensated by bucking coils to reduce the field at $L_{1,2}$ to about 1% of that applied at S so as to minimize the temperature changes due to remagnetization of the cooling salts. The gradients of the field in the region of the sample were adjusted carefully to give a signal as near to null as possible when the sample had zero moment. The solenoid was mounted on an earth's-field compensator-coil framework capable of reducing the residual field at the sample to less than 0.01 Oe.

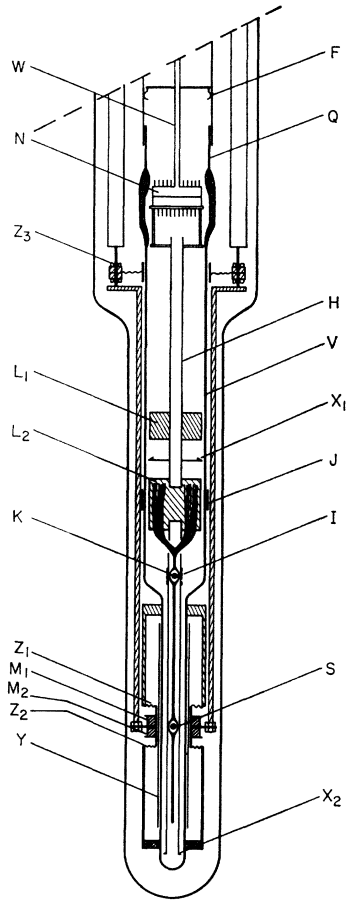

FIG. 1. Detail of vibrating-coil magnetometer—specimen mounting. Explanation in text.

B. Measurements

Specimens Nb10 and HR24 were cut from single crystals and ground to 3-mm-diameter spheres. Slabs roughly 10×3×1 mm also were cut from the larger samples in each case, and the resistivity and Hall coefficient of each was measured to determine n_c and the electronic mobility μ. The surfaces were cleaned but not polished.

The magnetic moments of the specimens were measured in fields up to H_{c2} in the temperature range 0.1°K to T_c. The measuring sequence involved was (1) adiabatic demagnetization of pills $L_{1,2}$; (2) vertical adjustment of the earth's field compensating coils and the external solenoid about the cryostat; (3) discharge of a capacitor through the specimen resistance heater to drive the specimen normal temporarily, thus removing trapped flux; (4) measurement of the paramagnetic thermometer (K, Fig. 1) temperature; and (5) measurement of the specimen magnetic moment versus applied field. Steps 3, 4, and 5 were repeated several times while cooling pill-thermometer-specimen assembly warmed to T_c over a period of several hours. The whole cycle could then be repeated as a check on reproducibility of the data.

On removal of magnetic fields greater than H_{c1}, each specimen exhibited a residual moment in the paramagnetic direction, indicating the presence of trapped flux. This property was used to determine H_{c1}; the magnitude of the residual moment was measured as a function of the highest applied field, and H_{c1} then can be identified as the highest field for which the residual moment is zero.[9]

[8] D. deKlerk and R. P. Hudson, J. Res. Natl. Bur. Std. 53, 173 (1954).

[9] This technique was kindly suggested to us by R. A. Hein of the Naval Research Laboratory, Washington. We thank Y. B. Kim, of Bell Telephone Laboratories, for pointing out that the technique was discussed by R. Hecht, contribution to the Cleveland Conference on Type-II Superconductivity 1964 (unpublished).

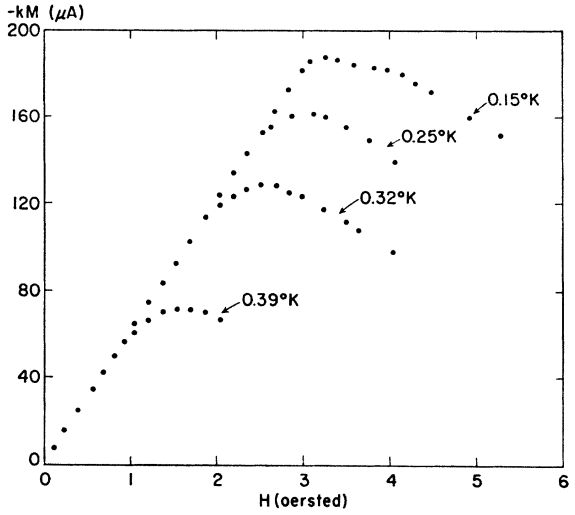

FIG. 2. Low-field magnetization of specimen Nb10.

The net stray heat leak to the specimen was measured by replacing it with a chrome potassium alum sphere and measuring warming rates. At 0.27°K the leak was 24 erg min^{-1} with the vibrator off and 32 erg min^{-1} with the vibrator operating at 0.5-mm amplitude. The vibrator settings used in these measurements were 23 cps and 0.5-mm amplitude. The paramagnetic thermometer K was calibrated against the He^4 bath vapor pressure from 1–2°K at the conclusion of each day's run, using the Curie-law extrapolation.[10]

Figures 2 and 3 show the parts of magnetization curves of Nb10 and HR24, respectively, at low applied fields, for a number of temperatures in the range $T=0.15$°K up to T_c. Figures 4 and 5 show complete magnetization curves and correspond with the curves shown in Figs. 2 and 3. The curves are similar in appearance and typical of type-II superconductors. The initial portion of the magnetization curve was shown to

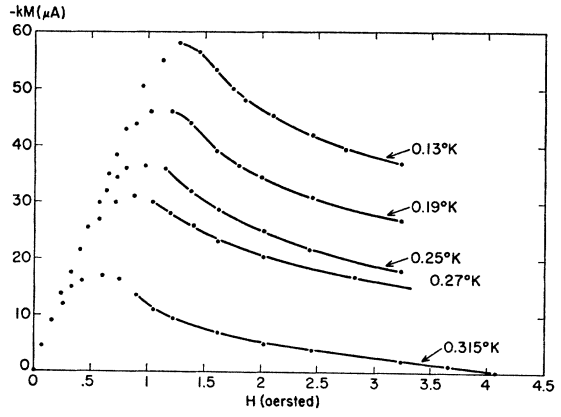

FIG. 3. Low-field magnetization of specimen HR24.

[10] See, for example, E. Ambler and R. P. Hudson, Rept. Progr. Phys. 18, 264 (1955).

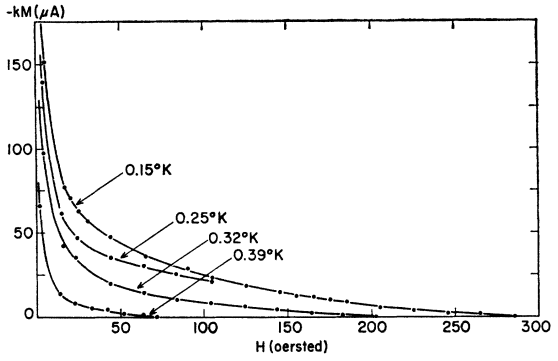

FIG. 4. Complete magnetization curves of specimen Nb10. Curves correspond to those in Fig. 2.

be linear with applied field with a slope corresponding to perfect diamagnetism within experimental accuracy, and to be reversible, indicating the applied field to be below H_{c1}. The rounding of the peak in the M-H curves is to be expected. Not only were the samples spherical in shape, but the magnetization above the peak was shown to be very irreversible indicating that the material is capable of trapping a very large moment.

Both the point of departure from linearity of the M-H curve and the limit to which H could be raised and lowered before a residual moment resulted (Fig. 6), were used to determine H_{c1}. The two methods agreed reasonably well. Values of H_{c1} were obtained for several temperatures and the results are displayed in Fig. 7 for Nb10 and Fig. 8 for HR24. The values of H_{c1} have been corrected to those appropriate for a needle-shaped specimen.[11]

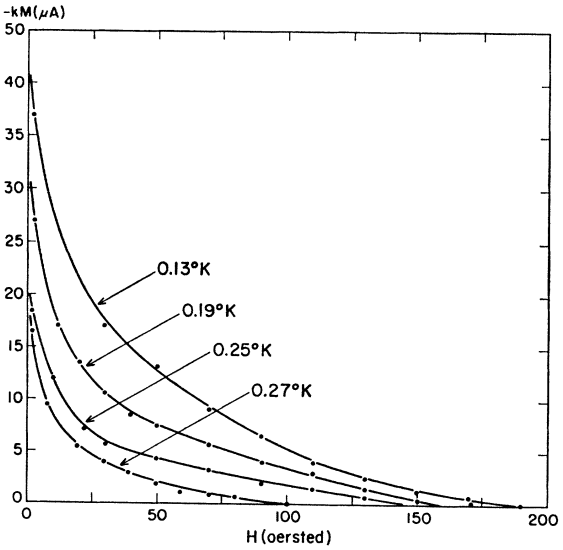

FIG. 5. Complete magnetization curves of specimen HR24. Curves correspond to those in Fig. 3.

[11] See, for example, E. Lynton, *Superconductivity* (Methuen and Company Ltd., London, 1962), p. 25.

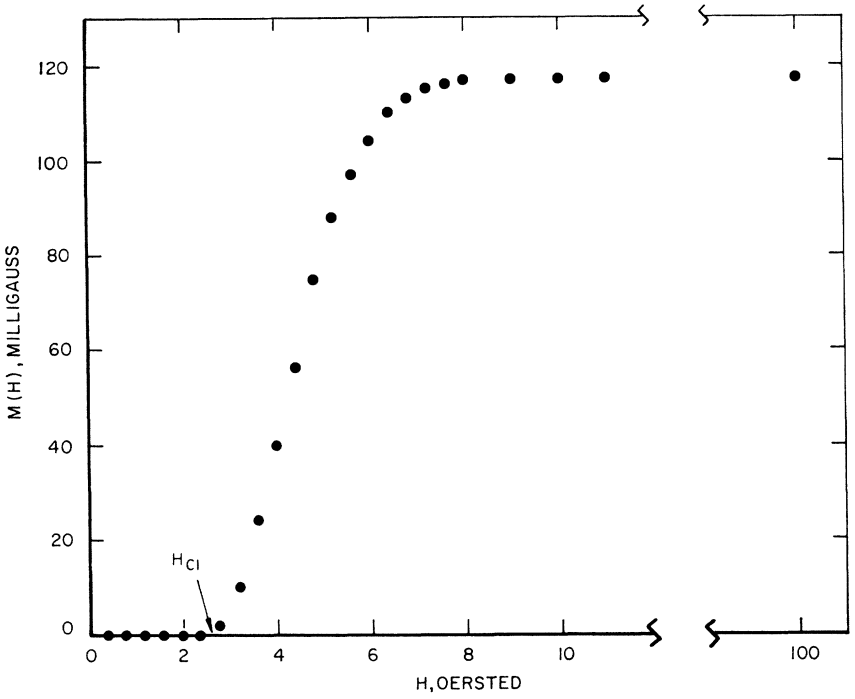

FIG. 6. Residual magnetic moment after removal of field H, for specimen Nb10, $T=0.2$°K.

TABLE I. Magnetization results, Nb10.

T (°K)	H_{c1} (corr) (Oe)	H_{c2} (Oe)	$\left[8\pi\int_0^{H_{c2}} M(T)dH\right]^{1/2}$ (Oe)
0	4.9 (calc)	504 (calc)	15 (est)
0.15	4.4	300	13.0
0.25	3.6	300	11.7
0.32	2.7	200	8.1
0.39	1.3	70	3.7
$0.43=T_c$	0.15	1.3	0.4

The values of H_{c2} were determined as the intercept of the M-H curve with the M axis. The small slope of the M-H curve at H_{c2} coupled with the greater experimental difficulties there (due to the difficulty of determining a null moment at relatively high measuring field) made the determination of H_{c2} accurate only to about 10%. These results are also shown in Figs. 7 and 8.

In addition to H_{c1} and H_{c2}, $H_c(M)$ (defined here in terms of the area under the magnetization curve)

$$\int_0^{H_{c2}} M(T)dH,$$

was determined at each temperature for which measurements were made. It should be noted that exact interpretation of $H_c(M)$ is difficult because of the magnetic hysteresis which is present. The results of all these measurements have been gathered together in Table I for Nb10 and Table II for HR24.

TABLE II. Magnetization results, HR24.

T (°K)	H_{c1} (corr) (Oe)	H_{c2} (Oe)	$\left[8\pi\int_0^{H_{c2}} M(T)dH\right]^{1/2}$ (Oe)
0	1.95 (calc)	420 (calc)	7.5 (est)
0.13	1.35	180	6.6
0.14	1.5	220	6.6
0.19	1.2	180	5.4
0.246	1.0	160	4.0
0.273	0.75	100	3.2
0.315	0.45	4	0.8
$0.33=T_c$			

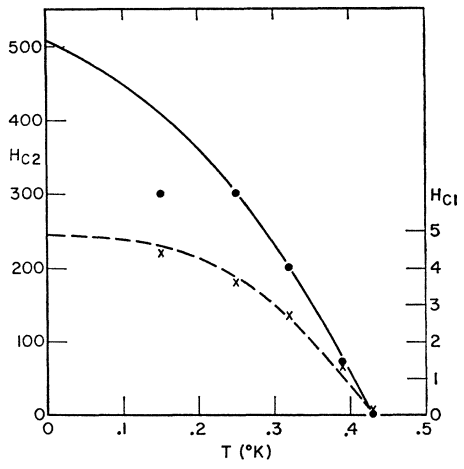

FIG. 7. $H_{c1}(T)$ (crosses), $H_{c2}(T)$ (solid circles), H_{c1} (calc) (dashed curve) and H_{c2} (calc) (solid curve) for specimen Nb10.

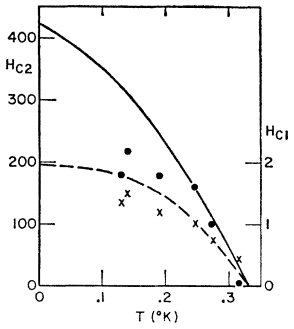

FIG. 8. $H_{c1}(T)$ (crosses), $H_{c2}(T)$ (solid circles), H_{c1} (calc) (dashed curve) and H_{c2} (calc) (solid curve) for specimen HR24.

III. HEAT-CAPACITY MEASUREMENTS

The heat capacity of specimen Nb13 was determined between 0.3 and 4°K. The specimen consisted of a 70 g polycrystalline boule doped during growth with Nb_2O_5. Because of the large size of the specimen the niobium doping level was expected to be somewhat nonuniform. Hall-effect measurements on slices taken from the ends and sides of the boule indicate the over-all carrier concentration to be in the range $n_c=1.4\pm0.3\times10^{20}$ cm^{-3}. Temperature measurements were made using a germanium resistance thermometer calibrated against the He^3 and He^4 vapor-pressure scales. The thermometer was sealed with Apiezon N grease into a thin-walled copper sheath which was soldered to the end of the $SrTiO_3$ boule with a small amount of indium. A heater of Evanohm wire was wrapped around the side of the boule and held in place with GE 7031 varnish. The assembly was supported by nylon threads which were tied and varnished to the sides of the boule. A mechanical heat switch which made contact with a small copper wire soldered to the thermometer sheath was used to cool the sample. The cryostat consisted of a He^3 refrigerator which has been described elsewhere.[12] A magnetic field could be applied to the specimen using a superconducting coil wrapped on the outer vacuum jacket of the cryostat.

The heat capacity between 0.5 and 4°K is represented within the experimental accuracy of 2% by the expression

$$C\ (\text{mJ deg}^{-1}\ \text{mol}^{-1})=1.60T+2.1\times10^{-2}T^3+9\times10^{-4}T^5. \quad (1)$$

The term linear in temperature is interpreted as the electronic contribution to the heat capacity, the coefficient $\gamma=1.60$ mJ deg^{-2} mol^{-1}=446 erg deg^{-2} cm^{-3}.

The results of the measurements below 1°K are shown in Fig. 9. Below 0.5°K the heat capacity deviates from that expressed by Eq. (1) as is shown in the figure, and the deviation is ascribed to the onset of superconductivity in the specimen. The data in Fig. 9 are the results of three separate runs between which the apparatus was warmed to 300°K. The measurements in a 260-Oe magnetic field were made during the final run. Between the second and third runs, the heat capacity of copper was measured to ensure that the observed deviation below 0.5°K was not due to errors in thermometer calibration. The heat capacities of the addenda (thermometer, heater, varnish, etc.) were calculated from the known quantities of materials used. This correction was less than 6% of the total heat capacity below 1°K and increased to 15% at 4°K.

A 1-cm o.d., 2-cm-long cylinder was cut from the same boule as Nb13, and the superconducting transition was observed by measuring the ac susceptibility at 210 cps and $H_{ac}\sim10^{-2}$ Oe. The transition occurred between $T=0.36$°K and 0.41°K. The ac transition was considerably broader than that characteristic of small single crystal specimens. Interpreting the sharp break in the heat capacity curve as the critical temperature gives $T_c=0.38$°K.

A second, but much smaller, break occurs in the heat-capacity curve at approximately 0.48°K. In the measurements made in the 260-Oe field the large increase in the heat capacity below 0.38°K is completely removed as expected; however, the smaller deviation below 0.48°K remains. It is possible that the deviation at 0.48°K is connected with the fact that specimens of $SrTiO_3$ show no electrical resistance up to temperatures some 0.1°K above the magnetic transition temperature.[6] The origin of this effect is not known with any certainty, although such effects are often ascribed to specimen nonuniformity.

The increase in the heat capacity at 0.38°K is not discontinuous, in contrast to theoretical type-II behavior.[13] This result, which is similar to that observed in the GeTe heat capacity,[14] could derive from inhomogeneous carrier concentration or from strains within the specimen. However, it should be noted that the measurements were made in the earth's field which is of the order of H_{c1} for the lowest temperatures reached in the experiment. The observed behavior may be an intrinsic property of SrTiO, resulting from the inability of the material to expel the magnetic field as it is cooled below T_c.

IV. DISCUSSION

From the γ value given by the heat-capacity measurements we can obtain at once the density of states at the Fermi surface, $N(E_F)$, through the relationship $N(E_F)=\frac{3}{2}\gamma/\pi^2k^2=7.96\times10^{30}\gamma$ cm^{-3} erg^{-1}. Thus we find for Nb13, $N(E_F)=3.56\times10^{33}$ states per cm^3 erg.[15]

[12] E. Ambler and R. B. Dove, Rev. Sci. Instr. **32**, 737 (1961).

[13] V. L. Ginzburg and L. D. Landau, Zh. Eksperim. i Teor. Fiz. **20**, 1064 (1950); A. A. Abrikosov, Zh. Eksperim. i Teor. Fiz. **32**, 1442 (1957) [English transl.: Soviet Phys.—JETP **5**, 1174 (1957)]; L. P. Gorkov, Zh. Eksperim. i Teor. Fiz. **37**, 1407 (1960) [English transl.: Soviet Phys.—JETP **10**, 998 (1960)].

[14] L. Finegold, Phys. Rev. Letters **13**, 233 (1964).

[15] This value is in excellent agreement with the density of states derived from measurements of the Seebeck coefficient (Ref. 2) and of the magnetic susceptibility. H. P. R. Frederikse and G. Candela, Phys. Rev. **147**, 583 (1966).

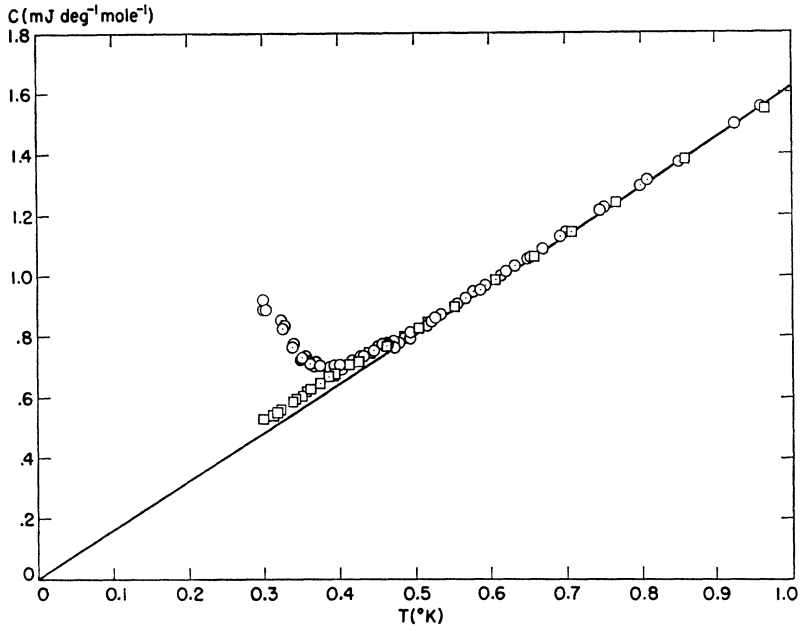

FIG. 9. Heat capacity of specimen Nb13 below 1°K in the earth's field (open circles) and in 260 Oe (open squares). The solid curve is given by Eq. (1).

Although the critical magnetic fields were not determined directly on Nb13 we can use the standard formula of the BCS model,[16] (approximately applicable to this case)

$$Hc^2/8\pi=\tfrac{1}{2}N(E_F)\Delta^2=0.234\gamma T_c^2 \qquad (2)$$

to obtain the thermodynamic critical field H_c. Taking $T_c=0.38$°K we obtain $H_c=20$ Oe at absolute zero.

The entropy change due to superconductivity in the specimen at 0.3°K can be calculated readily by integrating the quantity $[C(H=0)-C(H=260\text{ Oe})]/T$ between $T=0.30$°K and 0.38°K. The ratio of this quantity to $S_n=\gamma T$ at 0.3°K is 0.12. This ratio for an ideal superconductor at the same reduced temperature is 0.38. The substantial variation from the ideal ratio is not surprising considering the broadened nature of the superconducting transition in specimen Nb13. Coupled with the fact that the detectable impurity level is less than $\frac{1}{2}\%$, the observed entropy change offers direct evidence that superconductivity is a bulk phenomenon in $SrTiO_3$.

We have calculated the values of $H_c(0)$ for specimens Nb10 and HR24 using the Nb13 γ value adjusted for the respective differences in carrier concentration and using the experimentally determined transition temperatures. The values so obtained are 23.5 Oe for Nb10 and 16.5 Oe for HR24.

Examination of Figs. 7 and 8 shows that T_c is defined rather well by magnetic moment measurements. The presence of anomalous effects above T_c, as evidenced by the small deviation in the specific heat at 0.48°K (Fig. 2) and by electrical resistance measurements,[6] appear to be inconsequential as regards the specimen magnetic moment.

Maki[17] has recently derived expressions for the temperature dependence of H_{c1} and of H_{c2} as follows:

$$H_{c1}(T)=\sqrt{2}H_c(T)\ln\kappa_3(T)/2\kappa_3(T), \qquad (3)$$

$$H_{c2}(T)=\sqrt{2}\kappa_1(T)H_c(T). \qquad (4)$$

He has also calculated numerically the relations

$$[\kappa_3(T)/\kappa(T_c)] \text{ versus } (T/T_c)$$

and

$$[\kappa_1(T)/\kappa(T_c)] \text{ versus } (T/T_c),$$

where $\kappa(T_c)$ is just the Ginzburg-Landau κ appropriate at T_c. We have used these relations, together with the usual expression

$$H_c(T)=H_c(0)(1-T^2/T_c^2), \qquad (5)$$

to derive the values of $\kappa(T_c)$ and of $H_c(0)$ by fitting the experimental magnetization data, as shown in Figs. 7 and 8. In this procedure, more weight was given to the higher temperature measurements, since thermal gradi-

TABLE III. $H_c(0)$ values.

	$[2\pi\gamma T_c^2]^{1/2}$	Solution of Eqs. (3) and (4)	$\left[8\pi\int M(0)dH\right]^{1/2}$ (est)
Nb10	23.5	35.5	15.0
HR24	16.5	18.7	7.5

[16] J. Bardeen, L. N. Cooper, and R. Schrieffer, Phys. Rev. **108**, 1175 (1957).

[17] K. Maki, Physics **1**, 21, 127 (1964).

TABLE IV. Specimen parameters.

Specimen	$n_c(\times 10^{20}$ cm$^{-3})$	$\mu_{4.2°K}$ (cm^2 V^{-1} sec^{-1})	T_c (°K)	κ
Nb10	1.7	600	0.43	8.4
Hr24	1.0	225	0.33	13.2
Nb13	1.4	···	0.38	···

ents within the apparatus are expected to be lower at high temperatures. A better over-all fit could have been obtained by using somewhat lower values of $H_c(0)$ and κ. The solid line ($H_{c2}(T)$) and the dashed line ($H_{c1}(T)$) of Fig. 7 were calculated from Eqs. (3) and (4) using $H_c(0)=35.5$ Oe and $\kappa(T_c)=8.4$.

Similarly, for the calculated curves of Fig. 8, $H_c(0)=18.7$ Oe and $\kappa(T_c)=13$. The resulting values $H_{c1}(0)$ and $H_{c2}(0)$ for each specimen are noted in Tables I and II, and the quantities $H_c(0)$ appear in Table III. Table IV summarizes n_c, μ, T_c, and κ for the three specimens studied.

Examination of Table III shows that for each specimen, the value of $H_c(0)$ estimated from the integrations of the magnetization curves is substantially less than either calculated value. This is not unexpected, since the experimental data deviate from Eqs. (3) and (4) at the lower temperatures. This deviation suggests that the temperature dependence of Maki's κ values may be inappropriate in this case, although the possibility exists that the specimen temperature measurement may be inaccurate due to reduced thermal contact at lower temperatures.

The Maki relations were derived for superconducting alloys, where l, the electronic mean free path, is much less than the coherence length, $\xi_0=0.18(\hbar v_F/kT_c)$. The ratio l/ξ_0 for specimens Nb10 and HR24 is calculated to be approximately $(2\times10^{-6}$ cm$)/(1.6\times10^{-5}$ cm), satisfying Maki's criterion.

The ratio of κ(HR24) to κ(Nb10) is $13.2/8.4=1.5$, in qualitative agreement with the ratio μ(Nb10)/μ(HR24) $=2.5$, as would be expected from the relation

$$\kappa=(\lambda_L/\xi)\propto(\lambda_L/l)\propto\lambda_L/\mu \tag{6}$$

since $\xi^{-1}=\xi_0^{-1}+l^{-1}\approx l^{-1}$ for these specimens.

In conclusion it may be said that semiconducting $SrTiO_3$ appears to become a type-II superconductor at low temperatures, and that its κ value appears to be dependent upon the normal-state electronic mobility. The specimens measured show magnetic hysteresis; whether this property is intrinsic to high-κ materials, or is due for example to the strains which are seen in $SrTiO_3$ specimens below the 110°K phase transition[18] is an open question at present. Heat capacity measurements support existing evidence for a high density of electronic states[2,3,15,19] and for the nature of the superconducting state, in particular yielding values for T_c and $H_c(0)$.

ACKNOWLEDGMENTS

We are grateful to E. Roberts for preparation of the specimen Nb13 used in this investigation, to R. S. Kaeser and R. B. Dove for aid in construction of the magnetometer and to E. R. Pfeiffer for aid in the magnetic moment measurements. The continuing interest and advice of Professor M. L. Cohen and Dr. H. P. R. Frederikse in this work are also acknowledged with gratitude.

Certain commercial materials and equipment are identified in this paper in order to adequately specify the experimental procedure. In no case does such identification imply recommendation or endorsement by the National Bureau of Standards, nor does it imply that the material or equipment identified is necessarily the best available for the purpose.

[18] F. T. Lytle, J. Appl. Phys. **35**, 2212 (1964).
[19] H. P. R. Frederikse, W. R. Hosler, and W. R. Thurber, Phys. Rev. **143**, 648 (1966).